

# EMI RADIATION FROM SHIELDED SIGNAL CABLE INSIDE A SUBRACK

Ming Ye  
ERICSSON AB, Stockholm, Sweden  
ming.ye@era.ericsson.se

**Abstract:** This paper presents the analysis of EMI radiation (far-field) from a shielded cable installed inside a PCB sub-rack. The simulation analysis includes the two main parts, the EMI leakage penetrating through cable shield and the 3D full wave simulation of EMI radiation of the cable inside the subrack. FDTD method has been employed to perform the simulation analysis. The thin wire model implemented with the FDTD code is evaluated for the application to model the signal cables. Moreover, the simulated results have been validated through the comparison to measurement. The results show that the simulation method is applicable for EMC design of telecom products associating with EMI radiation from shielded cable assemblies.

## 1. Introduction

Signal transmission at high speed and high capacity (digital broadband) has been substantially increasing in mobile communication industry over recent years. EMI radiation due to signal transmission cables inside equipment cabinets is in particular one of critical issues for compliance of EMC requirement. It is recognized that these cable assemblies can be EMI sources to radiate electromagnetic field significantly because of signal transmission discontinuity happening between signal cables and terminal connectors. Thus one of the important tasks in telecom product design process is how to enable a prediction for EMI radiation (far-field) from an equipment during product design phase. From the view point of shielding electromagnetic field, the issue concerns with the two main parts: firstly individual assessment of the shielded cable SE (shielding effectiveness) and also equipment enclosure's SE (cabinet or subrack), and secondly 3D full wave analyse for spatial configuration of the shielded cables located inside the enclosure.

The paper describes the application of FDTD modelling technique to determine EMI radiation from a signal coaxial cable as it is placed inside a PCB (print-circuit board) sub-rack for installation of print-circuit boards. Briefly, the modelling procedure consists of the two steps: (1) to determine EMI leakage through signal

cable shield, and to represent signal cable as "thin wire" spatially configured inside FDTD volume, and (2) to perform the calculation of radiated electric fields by means of FDTD simulation that is implemented with the charged "thin" wire model. Moreover, the "thin" wire approach to a signal cable that is physically "thick" in diameter has been evaluated in the manner of varying the radiation gain. At last, the simulated results are verified by comparison of the measurement.

## 2. Theoretical description

In general, penetration of high frequency signals out of cable shield mainly includes EM field diffusion through solid metal part of cable shield and EM field leakages due to apertures on the shield. According to MTL (multi transmission line) theory, transmission characteristics of multiple core-conductors enclosed by cable shield, as illustrated in Figure 1, are formulated by the following matrix equations (1) and (2). Here the harmonic signal ( $e^{-j\omega t}$ ) is used.

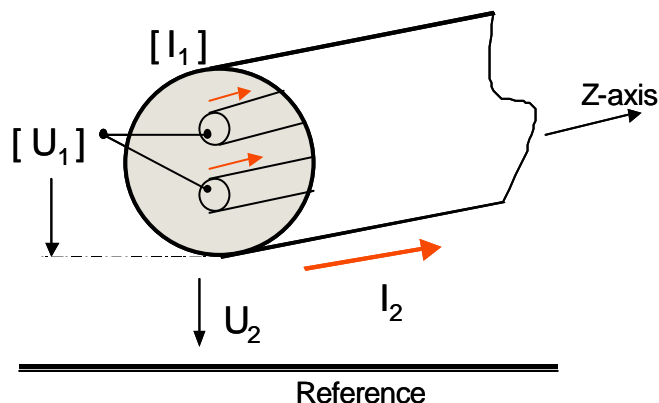


Fig. 1, Illustration of signal transmission through a shielded cable including multi-core conductors.

$$\begin{bmatrix} \frac{d\mathbf{U}_1}{dz} \\ \frac{dU_2}{dz} \end{bmatrix} = \begin{bmatrix} \mathbf{Z}_{11} & Z_{12} \\ Z_{21} & Z_{22} \end{bmatrix} \cdot \begin{bmatrix} \mathbf{I}_1 \\ I_2 \end{bmatrix} \quad (1)$$

$$\begin{bmatrix} \frac{d\mathbf{I}_1}{dz} \\ \frac{dI_2}{dz} \end{bmatrix} = \begin{bmatrix} \mathbf{Y}_{11} & Y_{12} \\ Y_{21} & Y_{22} \end{bmatrix} \cdot \begin{bmatrix} \mathbf{U}_1 \\ U_2 \end{bmatrix} \quad (2)$$

where the “bolded” letters,  $\mathbf{U}_1, \mathbf{I}_1, \mathbf{Z}_{11}$ , and  $\mathbf{Y}_{11}$  are respectively denoted as matrix vectors of voltage, current, impedance and admittance for the multi-core conductors inside cable shield. The letters not being “bolded” are of scalar variables to represent the characteristic impedance and admittance of cable shield, the voltage and current on cable shield. Obviously, equations (1) and (2) are valid to analyse signal transmission issue in 2D coordinate only. For the study purpose here, this approach is applicable to analyse signal transmission along multi-core wires enclosed by cable shield. When internal signals penetrate through cable shield, there will be electric charge distributed along the external surface of the cable shield. The electric charge acts as source to generate E and H fields in 3D space including complex geometry. To obtain the E and H fields is the matter of numerically solving Maxwell’s equations with arbitrary boundary conditions. The formula presentation on this matter is omitted here. Moreover, it is worth to note that in the analysis procedure the E and H fields outside cable shield are assumed not to affect the signal transmission inside cable shield.

- Magnetic leakage

From equation (1), voltage  $U_2$  and current  $I_2$  of the external surface of cable shield are driven by inner current  $\mathbf{I}_1$  (vector) through transfer impedance  $Z_T$  of cable shield. Here,  $Z_{12} = Z_{21} = Z_T$ . For a number of core conductors enclosed inside cable shield, the current on internal surface of cable shield equals the sum of currents of all core conductors. The EMI voltage source per unit length (V/m) due to magnetic leakage is expressed by,

$$U_{EMI} = Z_T \cdot \left( \sum_{k=1}^n I_k \right) \quad (3)$$

n: number of core-conductors. For a coaxial cable, the voltage EMI source per unit length (V/m) is formulated as:

$$U_{EMI} = Z_T \cdot I_1 \quad (4)$$

- Electric leakage

Similarly, equation (2) indicates that current  $I_2$  and voltage  $U_2$  on the external surface of cable shield are also driven by inner voltage  $\mathbf{U}_1$  (vector) through transfer admittance  $Y_T$  of cable shield. Here,  $Y_{12} = Y_{21} = Y_T$ . For a number of core conductors inside cable shield, the current EMI source per unit length is written,

$$I_{EMI} = \left( \sum_{k=1}^n Y_T \cdot U_k \right) \quad (5)$$

n: number of core-conductors. For a coaxial cable, the current EMI source per unit length (A/m) is formulated by:

$$I_{EMI} = Y_T \cdot U_1 \quad (6)$$

### 3. Cable simulation set-up

A time domain code for cable harness modelling has been employed to determine both electric and magnetic leakage sources of cable shield,  $U_{EMI}$  and  $I_{EMI}$ . Excitation is a voltage Gaussian impulse between core conductor and shield at the down end of the cable. Both ends of the core conductor are matched with 50  $\Omega$  impedance. The transfer impedance and admittance of RG-58 cable shield are determined by the formula (5.39) and (5.44) given in reference [2]. In HF range, the approach can be made that the diffusion term of the transfer impedance are neglected for its value so low. Figure 2 presents the waveforms of excitation Gaussian impulse, the voltages through out the shield at the starting and middle points

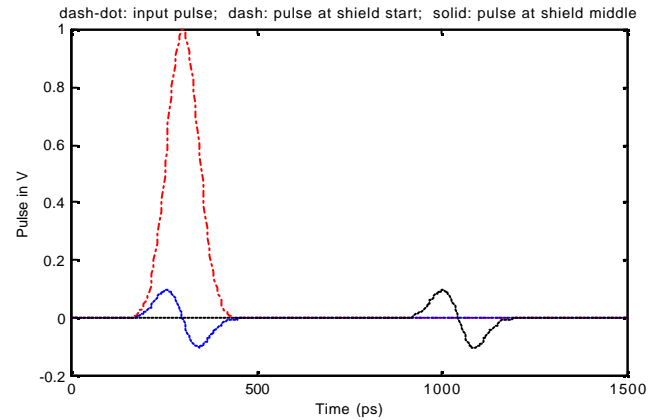


Fig. 2, Waveforms of the Gaussian impulse (dash-dot line) at sending end of cable core conductor and the voltage sources along the cable shield at the 1<sup>st</sup> (dashed line) and at the 10<sup>th</sup> section (solid line) of the “thin” wire.

### 4. FDTD simulation set-up

FDTD model of the sub-rack includes a number of simplifications in comparison with a practical sub-rack that includes many small circular holes, thin metal bars, and junctions with a number of screws. Regarding to the highest frequency of interest, say 2 GHz (a wavelength of 15 cm), these fine details mentioned may not

contribute significantly to the results but takes much longer computation time if including the fine detail in modelling. One has to accept some kind of physical approach to the studied object. To be effective in computation, thus, FDTD model treats all of the plates of the sub-rack as perfect conductive plates, and all of the plate junctions matched perfectly without screws presented, see Figure 3. The vertical wire has a radii of 0.1 mm in direct connection between upper and down plates of the sub-rack. The size of FDTD unit cell is selected as  $3 \times 3 \times 2$  ( $\Delta x \cdot \Delta y \cdot \Delta z$ ) mm<sup>3</sup>. The first order Mur boundary condition with Fang-Mei correction is selected as PML (Perfect matched layer) of the FDTD volume. For calculate of far fields, the visual surface is created at a interval of two unit cells inner the PML boundary to be an equivalence to the FDTD volume. The observation of far fields around the sub-rack is defined, shown in Fig. 4. Excitation of the vertical wire is given by equations (4) and (6), the EMI voltage and current sources per unit length along the wire, respectively. Waveform of the voltage source at two different places are presented in Fig. 2.

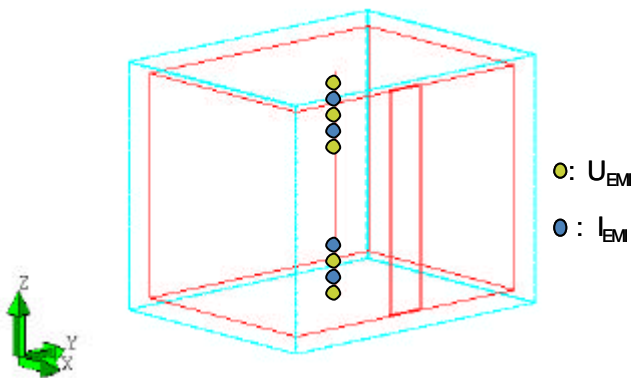


Fig. 3, Illustration of FDTD model for EMI radiation of a shielded cable inside the sub-rack

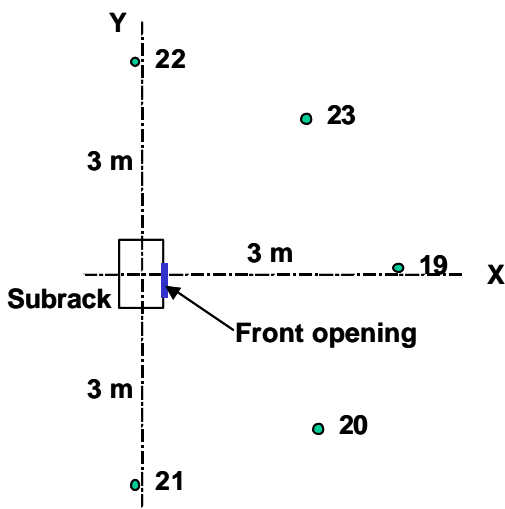


Fig. 4, Top view of Efield observation at points 19 to 23 at 3 m distance from the cable in sub-rack. 0 degree starts from X-axis.

The computation stability is ansured with the following of FDTD stability condition. The time step is therefore selected to 3.2 ps. The number of computing time step is 40000 to have 128 ns time window that gives a frequency step of about 7.8 MHz by Fourier transformation in frequenc domain. This resolution is enough accurate for observing the interesting phnomana in the frequency range from 100 MHz to 10 GHz.

### 5. Assessment of thin wire model

A wire considered to be “thin” is due to the wire radii much smaller than the FDTD unit cell length. Theoretically, the radii of thin wire should be ranged in 0.33% - 33% of the length of FDTD unit cell [2]. Higher the percentage to be a “thick wire” may cause instability of FDTD computation process. Some of the previous researchers have verified the thin wire model through comparing between FDTD and MoM (Method of moment) simulations [3]. In their verification it has been shown that the radii of “thin” wire can be selected up to 20% of the unit cell length. The error due to the “thick” wire is less than 4%. However, the problem is that even with this approaching and stable numerical computation the thin wire radii to a large extend is still much smaller than the cable outer radii in practice. Thus uncertainty does exist to model a practical cable as a “thin” wire. Care has to be taken for the error level caused by the uncertainty if it is tolerable. Thus it is necessary to evaluate the possible caused errors before applying the thin wire model for modelling practical cables.

This evaluation has been carried out by running a full wave MoM simulation in frequency domain. As the model shown in Figure 5, a vertical wire is placed in the same way as the cable location inside the subrack. The different radii of the wire are selected in the evaluation. The outer radii of RG-58 cable is 2.5 mm, and the radii of the thin wire is selected to 0.1 mm that equals to 5% of the minimum length of the unit cell. The excitation source is located at the bottom end of the wire, and has

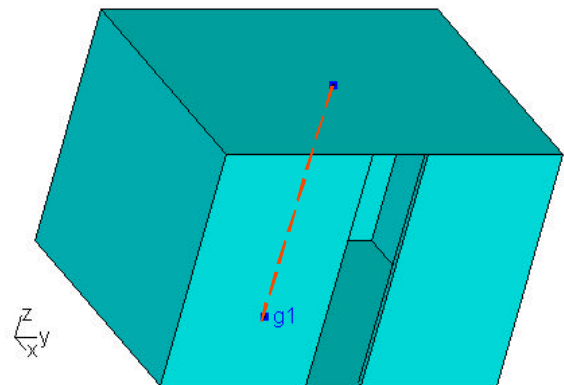


Fig. 5, MoM model for verifying the “thin wire” approach. The wire is placed inside the subrack and the excitation source ( $U_s=1.0$  Vrms) is placed at the bottom end of the wire.

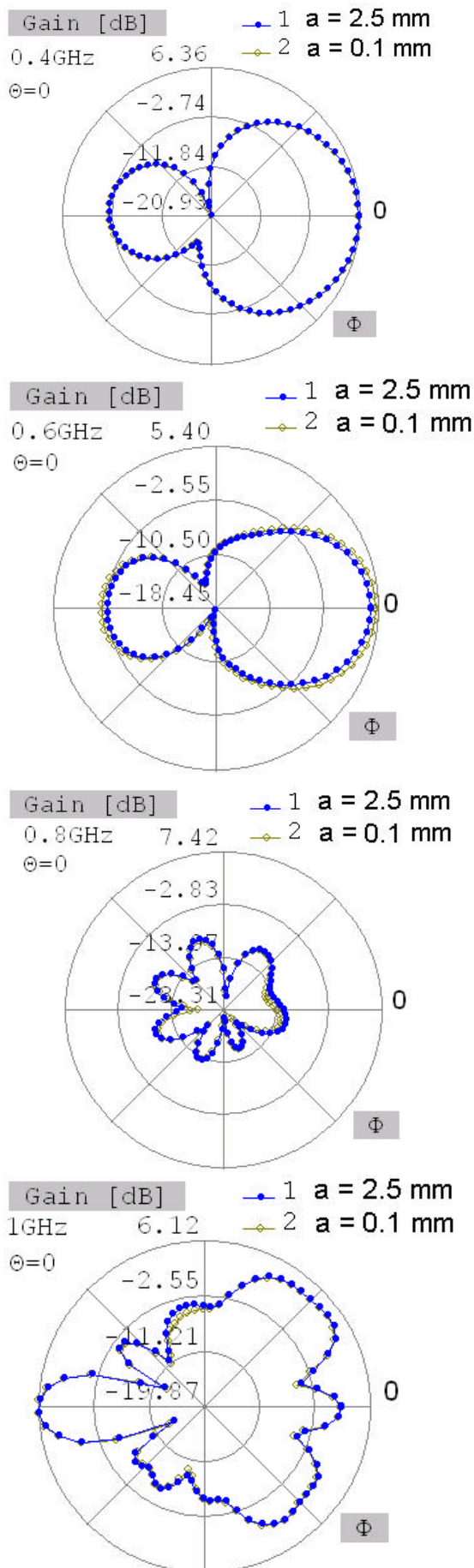


Figure 6, Electric field radiation Gain (dB) via azimuth  $\phi$  for elevation  $\theta = 0$ , where  $a$  is the wire radii.

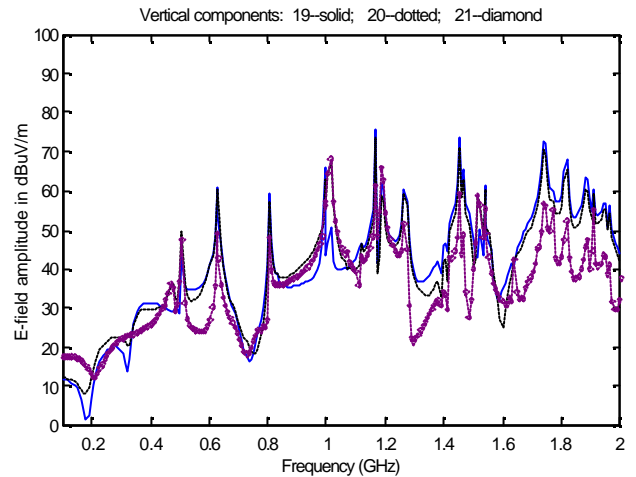


Fig. 7, Vertical components of electric fields at observing points 19 through 21

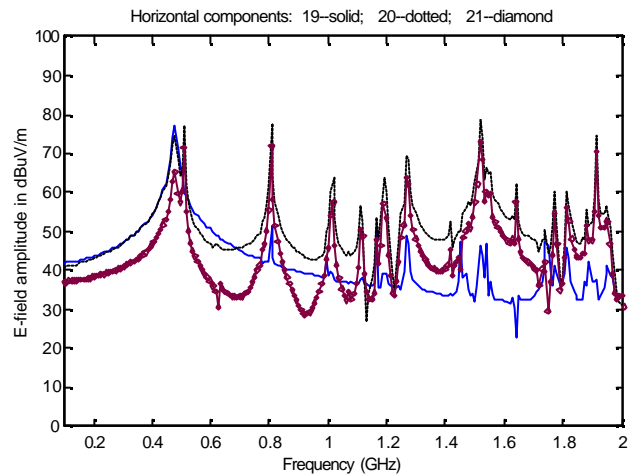


Fig. 8, Horizontal components of electric fields at observation points 19 through 21.

the amplitude of 1.0 Vrms. The excited subrack may perform as a kind of antenna array. The gain pattern of EM-field radiation from the subrack is selected to be a measuring parameter for evaluation of the wire to be "thin or "thick". Figure 6 shows the gain pattern as the wire radii to be 2.5 mm and 0.1 mm, respectively. With the results shown in the figures, the error level is limited less than 1 dB in all directions in a quite broad frequency range. The approximation of thin wire model for cable is therefore acceptable. The results can be explained that physically, the variation of the wire radii is in the range relatively much smaller than the spatial distance between the wire and the nearest plates of the sub-rack. So, the signal cable is like a "thin wire" from the viewpoints of its location and the size of sub-rack

## 6. Simulation results

The calculated electric fields are presented in a cylinder coordinate to be the same coordinate as measurement for further validation of the simulation results. Next, the simulated results have to be normalized to 0 dBm excitation input signal. Presentation for the simulated electric fields includes the vertical and horizontal

components of the electric fields at all three observation points 19 through 21, see those curves in Figures 7 and 8, respectively. Because of the resonance happened at a number of frequencies, the amplitudes of those electric fields are varying significantly between 35 and 95 dBuV/m for its horizontal components, and between 5 and 90 dBuV/m for its vertical components. In principle, the resonant frequency is partly due to the subrack cavity resonance, and partly due to the cable, the “thin” wire, resonance.

## 7. Validation

Simulation model validation are known as the most time-consuming tasks, which associates with computation stability, boundary conditions, quantitative error measures and so on. In a number of ways to validate the simulation results, the normal and traditional way for validation, which will be the procedure to compare the simulated results with measurement, is selected. For this reason, the measurement of the RF radiation from the shielded cable have been performed

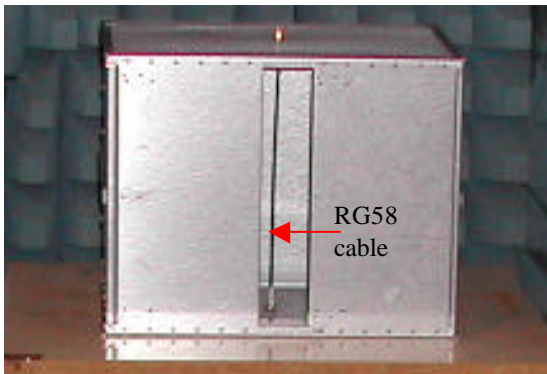


Fig. 9, a subrack installed with RG-58 coaxial cable inside. The opening at front is 60 mm

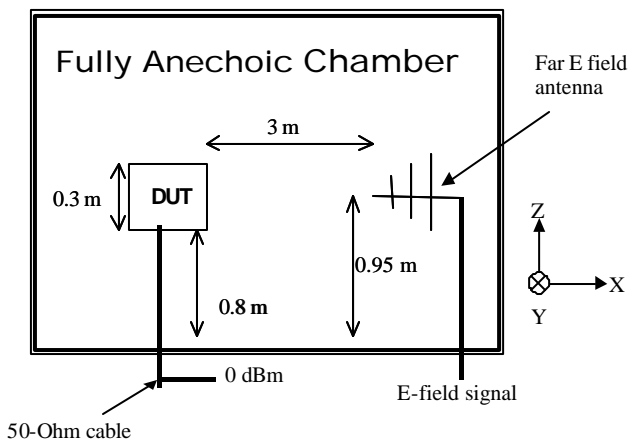


Fig. 10, Set-up (side view) for the measurement of electrical fields at 3 m distance from DUT.

- Measurement description

The selected DUT (device under test) is a subrack that has the same geometry size as the simulation model; see Figure 9. The plates on the top and the bottom of the DUT are the type of shielding net made of the material of Alu-Zink alloy. The rest of the subrack plates are the solid type also made of Alu-Zink alloy. The RG-58 coaxial cable is installed inside, which is a matched by 50 Ohm in SMA type at the DUT top plate. The excitation signal is sent through 50-Ohm signal cable to the bottom end of the RG-58 cable. The measurement has been performed in FAC (Fully Anechoic Chamber) room, see the set-ups in Figure 10. The DUT is placed on the wooden turning table 0.8 m high from ground level. The far-field antenna is located at a distance of 3 m to the DUT and a height of 0.9 m from ground. The level of excitation signal at the feeding cable output is 0 dBm, which is corresponding to 1.0 mW on the 50 Ohm output of the feeder cable. This power contributes to the input signal voltage of 0.224 Vrms. The measurement frequency is ranged from 0.1 to 1.25 GHz at the uniform frequency interval of 0.34 MHz.

- Differences between model and DUT

Note that in comparison to the DUT the simulation model is relatively rough due to a lot of differences existed. Many fine details such as the screws, the junctions and plate materials of the DUT are neglected in the simulation model. Thus, all of the differences are treated as the assumptions included in the simulation model.

- Comparison

The observation of the measurement covers all of the points specified in Figure 4, which are comparable. To

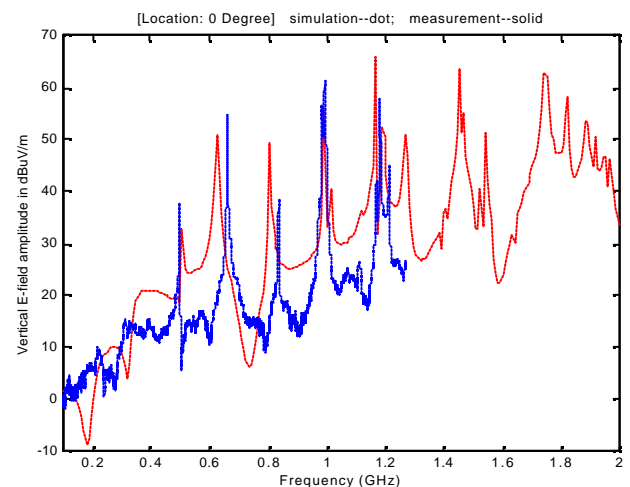


Figure 11, Measured and simulated vertical components of the electric fields observed at point 19, 0 degree to x-axis. Dotted line for simulation and solid line for measurement.

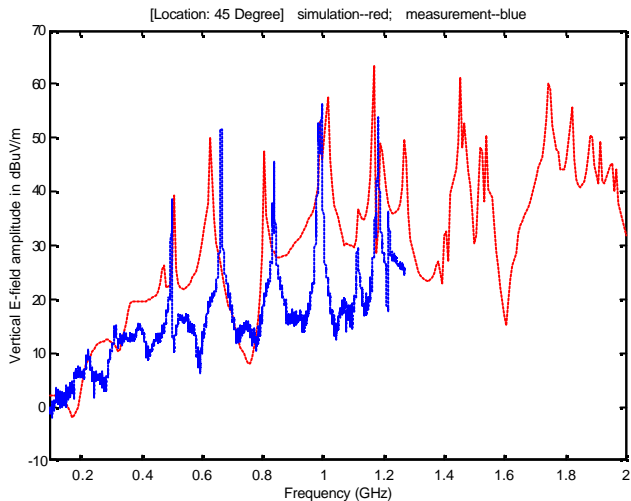


Fig. 12, Measured and simulated vertical components of the electric fields observed at point 20, -45 degree to  $x$  axis. Dotted line for simulation and solid line for measurement.

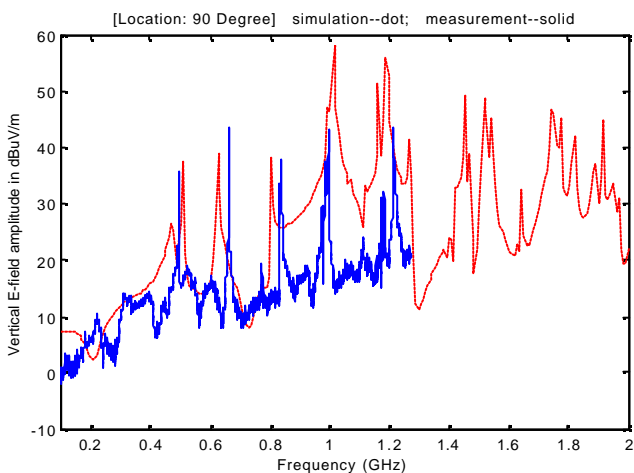


Fig. 13, Measured and simulated vertical components of the electric fields observed at point 21, -90 degree to  $x$  axis. Dotted line for simulation and solid line for measurement.

the limit of the article length, only parts of the comparison are selected in presentation. They are the vertical electrical field components at observation points 19 (0 degree), 20 (-45 degree), and 21 (-90 degree), respectively. They are exhibited in Figures 11, 12 and 13, respectively. Note that in those figures the curves are compared in the case of different frequency steps, 7.8 MHz for simulation and 0.34 MHz for measurement. With an outline view of the results, the assumption for the loss-less wire and subrack may cause higher electric field amplitude in the simulation than in the measurement. The small shift of the resonant frequencies above 500 MHz are observed, which is typical phenomena due to the different effects from free space in simulation and also the FAC environment in measurement. Nevertheless, the simulation method have at a high reliability predicted the significant resonant frequencies and the amplitude of the radiated

E-fields, which are the most important parameters for enclosure's EMC design.

## 8. Conclusions

In summary of the study, the conclusions may be drawn as the following points,

Hybrid-application of FDTD simulation and cable harness simulation has been successfully performed to analyse the EMI radiation of the shielded signal cable located in an enclosure that is physically complicated.

The results in both simulation and measurement are fairly agreed each other, even they are not exactly matched. This means that the theoretical approximation for the shielded cable EMI leakage and the simulation methods are of valid tools to predict the EMI radiation of shielded cable located in a complex EM environment.

The "thin wire" model for application of the "thick" shielded signal cable has evaluated. The approach is applicable and accurate for this set-up.

Accuracy of FDTD simulation depends on physical model construction for the DUT. This is an approaching procedure from physical object to its simulation model. More detail approaching to reality more accurate, but it takes more simulation time. It is obvious that effective simulation is the best for engineering practice, which results in the shorter simulation time and fairly reasonable accuracy enough for product EMC design.

## 9. Acknowledgement

I would like to thank Per Sjöberg for his help in acquisition of the measurement results. Thanks also to Hong Tang for his valuable suggestions on this study.

## 10. References

- [1] Taflove, A., "Computational electrodynamics, - the finite-difference time -domain method", Artech House, 1995.
- [2] Vance, E. F., "Coupling to shielding cables", John Wiley-sons Inc., 1978.
- [3] Hockanson, D. M., Drewniak, L. T. and et al, "FDTD Modeling of Common-Mode Radiation from Cables", IEEE trans. On EMC, Vol 38 - 3, pp376 - 386, 1996.
- [4] Ye, M. "Validation for FDTD and MoM simulations for EMC hardware design", Ericsson internal report, 2002.

## Contact address:

Dr. M. Ye  
EMC, Signal Integrity, Overvoltage Protection  
Dept. of system properties technology  
ERICSSON  
Arnborstvagen 14, Alvsjo, Stockholm  
SE-126 25, SWEDEN  
E-mail: ming.ye@era.ericsson.se